

## Ni(II) coordination compounds based on mixed phthalate and aromatic amine ligands: synthesis, crystal structures and magnetic properties

Svetlana G. Baca<sup>a,\*</sup>, Irina G. Filippova<sup>b</sup>, Patrik Franz<sup>c</sup>, Christina Ambrus<sup>c</sup>,  
Maria Gdaniec<sup>d</sup>, Helen Stoeckli-Evans<sup>e</sup>, Yurii A. Simonov<sup>b</sup>, Olese A. Gherco<sup>b</sup>,  
Tanea Bejan<sup>a</sup>, Nicolae Gerbeleu<sup>a</sup>, Silvio Decurtins<sup>c</sup>

<sup>a</sup> Institute of Chemistry, Academy of Sciences of RM, MD-2028 Chisinau, Republic of Moldova

<sup>b</sup> Institute of Applied Physics, Academy of Sciences of RM, MD-2028 Chisinau, Republic of Moldova

<sup>c</sup> Department of Chemistry and Biochemistry, University of Berne, CH-3012 Berne, Switzerland

<sup>d</sup> Faculty of Chemistry, A. Mickiewicz University, 60-780 Poznan, Poland

<sup>e</sup> Institut de Chimie, Université de Neuchâtel, CH-2007 Neuchâtel, Switzerland

Received 10 March 2004; accepted 24 October 2004

Available online 19 November 2004

### Abstract

Three new coordination compounds,  $[\text{Ni}(\text{Pht})(\text{Py})_2(\text{H}_2\text{O})_3]$  (**1**),  $[\text{Ni}(\text{Pht})(\beta\text{-Pic})_2(\text{H}_2\text{O})_3] \cdot \text{H}_2\text{O}$  (**2**) and  $[\text{Ni}(\text{Pht})(1\text{-MeIm})_2(\text{H}_2\text{O})_3]$  (**3**) (where  $\text{Pht}^{2-}$  = dianion of *o*-phthalic acid; Py = pyridine,  $\beta\text{-Pic}$  = 3-methylpyridine, 1-MeIm = 1-methylimidazole), have been synthesized and characterized by IR spectroscopy and thermogravimetric analysis. Crystallographic studies **1–3** reveal that each Ni(II) center has a distorted octahedral geometry being coordinated by two nitrogen atoms of aromatic amines, one oxygen atom from a carboxylate group of a phthalate ligand and three water molecules.  $\text{Pht}^{2-}$  anions act as monodentate ligands, while the remaining uncoordinated carboxylate oxygen atoms participate in the formation of hydrogen bonding. The uncoordinated oxygen atoms form hydrogen bonds with the coordinated water molecules from adjacent complexes creating a centrosymmetric dimer unit. Further, these dimer units are connected by O–H···O hydrogen bonds in double-chains. Depending on the nature of aromatic amines, the arrangement of these double-chains differs. The double-chains are held together only by van der Waals interactions in **1**. In contrast, in **2** these chains form layers by  $\pi$ – $\pi$  interactions between antiparallel molecules of  $\beta\text{-Pic}$  as well as by  $\pi$ – $\pi$  interactions between  $\beta\text{-Pic}$  and Pht aromatic rings. In complex **3**, the double-chains are knitted together via C–H···O hydrogen bonds between the methyl group of 1-MeIm and the coordinated carboxylate oxygen atom of Pht, as well as  $\pi$ – $\pi$  contacts involving antiparallel 1-MeIm cycles. The thermal dependence of the magnetic susceptibilities for compounds **1** and **2** shows a weak antiferromagnetic interaction between the two  $\text{Ni}^{2+}$  ions of the hydrogen bonded dimers. For compound **3**, a ferromagnetic interaction could be observed. Modeling the experimental data with MAGPACK resulted in:  $g = 2.22$ ,  $|D| = 4.11 \text{ cm}^{-1}$  and  $J = -0.29 \text{ cm}^{-1}$  for compound **1**,  $g = 2.215$ ,  $|D| = 3.85 \text{ cm}^{-1}$  and  $J = -0.1 \text{ cm}^{-1}$  for compound **2** and  $g = 2.23$ ,  $|D| = 4.6 \text{ cm}^{-1}$  and  $J = 0.22 \text{ cm}^{-1}$  for compound **3**. © 2004 Elsevier B.V. All rights reserved.

**Keywords:** Nickel(II) compounds; Carboxylates; Phthalate complexes; Crystal structures; Magnetic properties

### 1. Introduction

*o*-Phthalate anion is a well-known versatile ligand, which has been extensively used in the design of coordination compounds due to a variety of its bonding abili-

\* Corresponding author. Tel.: +373 22 72 5490; fax: +373 22 73 9954/9611.

E-mail address: [sbaca\\_md@yahoo.com](mailto:sbaca_md@yahoo.com) (S.G. Baca).

ties. As a result of the two *ortho*-carboxylic groups, the ligand has the capacity to chelate as well as to bridge up to seven metal centers at once [1, Scheme 1] forming mono- and polynuclear complexes. Based on analysis of the crystal structures of phthalates extracted from the Cambridge Structural Database (CSD) [2] in our previous report [1], we have shown that the phthalate ligand can adopt 26 coordination modes with metal atoms in the complexes. Moreover, both monodeprotonated  $\text{HPht}^-$  anions and neutral  $\text{H}_2\text{Pht}$  molecules are able to co-exist with fully deprotonated  $\text{Pht}^{2-}$  residues of acid in crystals, leading to some unexpected architectures. In particular, we previously described an extremely unusual dimer  $[(\text{bpy})_2\text{Zn}(\text{Pht})\text{H}(\text{Pht})\text{Zn}(\text{bpy})_2](\text{HPht})(\text{H}_2\text{Pht}) \cdot 2\text{H}_2\text{O}$  in which  $[\text{Zn}(\text{bpy})_2]$  metal cores are connected through  $\text{Pht} \cdots \text{H} \cdots \text{Pht}$  bridge [3]. Additional strong hydrogen bonds between water molecules and coordinated and uncoordinated moieties of *o*-phthalic acid as well as  $\pi$ - $\pi$  interactions between uncoordinated phthalate moieties and one of bpy molecule stabilize the structural organization of this complex.

However, the 1,6-bridging mode remains the most commonly seen in the complexes. In this case, the phthalate anion is a bidentate ligand and coordinates to metal ions by one oxygen atom from each of the carboxylate group. This structural motif of the ligand promotes the formation of polymeric structures such as were found in copper(II) [4–9], cobalt(II) [10–12], zinc(II) [13–15] and other metal complexes [16]. It is noteworthy that when the 1,6-bridging mode is realized, the other oxygen atoms from the same carboxylate groups are also able to coordinate additional metal ions resulting in supracage assemblies or complicated polymeric structures. The good examples of the former are the fascinating  $\text{Mn}_{18}$  [17,18] and  $\text{Mn}_{10}$  [19] clusters reported by Christou et al. as well as Winpenny's remarkable  $\text{Ni}_{16}$  [20] and  $\text{Co}_{13}$  [21,22] cages, which contain phthalate ligands displaying rare and unprecedented bridging modes. For the latter case, we can mention the coordination polymer  $[\text{Zn}(\text{Pht})(2\text{-MeIm})_n]_n$  [15]. In this structure, one of a pair of zinc atoms is linked by 1,6-bridges of two phthalate ligands, while the other is held together through *syn-syn* bridging carboxylate groups in a 1,3-fashion from the same phthalates. As a result, infinite chains with alternation of 14- and 8-membered cycles are formed. All these structural and functional versatilities make phthalate ligand an attractive building unit in the construction of metallopolymers and clusters. The coordination of residues of  $\text{Pht}^{2-}$  or  $\text{HPht}^-$  by only one carboxylate group to metal ions is also of special interest, since the uncoordinated carboxylic group can be important in different catalytic processes [23].

We have focused our efforts on synthesis and investigation of 3d coordination compounds based on mixed phthalate ligand and aromatic amines such as pyridine,

imidazole and their derivatives and several interesting cobalt(II), copper(II) and zinc(II) [1,3,8,12,14,15] complexes have been prepared in our laboratory. However, despite the characterization of many new complexes of 3d-metals with *o*-phthalic acid, little work has been done to synthesize nickel(II) compounds. A search of the Cambridge Structural Database (CSD version 5.24 [2]) yielded only 11 structural investigations of Ni(II) complexes with the phthalate ligand. It should be noted that in six of them the moiety of phthalate is monodentate. Examples of such mononuclear Ni(II) complexes include  $[\text{Ni}(\text{HPht})_2(\text{H}_2\text{O})_4] \cdot 2\text{H}_2\text{O}$  [24] and  $[\text{Ni}(\text{Pht})(\text{ethylenediamine})_2(\text{H}_2\text{O})]$  [25]. Polletti et al., using chelating N,N-ligands such as 1,10-phenanthroline, 2,2'-bipyridine, and bipyridilamine, synthesized mononuclear Ni(II) phthalate complexes with common formula  $[\text{Ni}(\text{Pht})(\text{A})(\text{H}_2\text{O})_3] \cdot n\text{H}_2\text{O}$  (where A = 1,10-phenanthroline,  $n = 1$  [26]; bipyridylamine,  $n = 2$  [26]; 2,2'-bipyridine,  $n = 1$  [27]), as well as a similar complex  $[\text{Ni}(\text{Pht})(\text{bpy})(\text{H}_2\text{O})_3] \cdot \text{C}_2\text{H}_5\text{OH} \cdot \text{H}_2\text{O}$  but containing an additional solvate ethanol molecule [28]. In  $\{[\text{Ni}(\text{Pht})(\text{oxamide oxime})_2] \cdot 4\text{H}_2\text{O}\}_n$  [29] and the above-mentioned  $\text{Ni}_{16}$  cluster  $[\text{Ni}_{16}\text{Na}_6(\text{chp})_4(\text{Pht})_{10}(\text{HPht})_2(\text{MeO})_{10}(\text{OH})_2(\text{MeOH})_{20}]$  [20], the Pht moieties act as bridges and enhance the formation of a linear polymer in the first case and the supercage structure in the second one. In the latter case, the bridge is realized between  $\text{Ni}^{2+}$  and  $\text{Na}^+$  ions. In  $\text{K}_2[\text{Ni}(\text{H}_2\text{O})_6](\text{HPht})_4 \cdot 4\text{H}_2\text{O}$  [30],  $[\text{Ni}(\text{bpy})_3]_2(\text{HPht})(\text{NO}_3)_3 \cdot 4\text{H}_2\text{O}$  [31] and  $[\text{Ni}(1\text{-MeIm})_6](\text{HPht})_2 \cdot 2\text{H}_2\text{O}$  [1], phthalate does not take part in coordination to nickel ions and it coordinates to  $\text{K}^+$  ions in the first case and plays the role of counter anions in the latter. Analyzing these data, we can consider the monodentate coordination of the phthalate ligand as the most favored for the nickel(II) complexes with *o*-phthalic acid.

In this paper, we report on the synthesis, characterization and crystal structures of three new nickel(II) phthalate compounds:  $[\text{Ni}(\text{Pht})(\text{Py})_2(\text{H}_2\text{O})_3]$  (1),  $[\text{Ni}(\text{Pht})(\beta\text{-Pic})_2(\text{H}_2\text{O})_3] \cdot \text{H}_2\text{O}$  (2) and  $[\text{Ni}(\text{Pht})(1\text{-MeIm})_2(\text{H}_2\text{O})_3]$  (3) (where  $\text{Pht}^{2-}$  = dianion of *o*-phthalic acid; Py = pyridine,  $\beta\text{-Pic}$  = 3-methylpyridine, 1-MeIm = 1-methylimidazole).

## 2. Experimental

### 2.1. Materials and physical measurements

All reagents were purchased from commercial sources and used as received.  $[\text{Ni}(1\text{-MeIm})_6](\text{HPht})_2 \cdot 2\text{H}_2\text{O}$  was prepared by the reported procedure [1]. IR spectra were recorded on a Perkin-Elmer Spectrum One spectrometer in the region  $4000\text{--}400\text{ cm}^{-1}$  using KBr pellets. TG analyses were carried out on a Mettler-Toledo TA 50

in dry nitrogen ( $60 \text{ ml min}^{-1}$ ) at a heating rate of  $5 \text{ }^\circ\text{C min}^{-1}$ .

## 2.2. Synthesis of complexes

### 2.2.1. Synthesis of $[\text{Ni}(\text{Pht})(\text{Py})_2(\text{H}_2\text{O})_3]$ (**1**)

To a hot solution of  $\text{H}_2\text{Pht}$  (0.83 g, 5 mmol) and pyridine (3 ml) in water (30 ml) was added a solution of  $\text{Ni}(\text{O}_2\text{CCH}_3) \cdot 4\text{H}_2\text{O}$  (1.24 g, 5 mmol) in water (10 ml). The mixture was heated at reflux for 1 h and left to stand at r.t. in an open flask. The precipitated blue crystalline product was collected by filtration, washed with water, EtOH and Et<sub>2</sub>O and dried in air. Yield: 1.71 g, 78.62%. *Anal. Calc.* for  $\text{C}_{18}\text{H}_{20}\text{N}_2\text{NiO}_7$ : C, 49.69; H, 4.63; N, 6.44. Found: C, 49.66; H, 4.67; N, 6.41%. IR data (KBr,  $\text{cm}^{-1}$ ): 3209s,br, 1607vs, 1586sh, 1563vs, 1488s, 1449s, 1404vs, 1219m, 1153m, 1084w, 1072s, 1043s, 1015m, 951m, 932m, 887m, 812s, 761s, 698s, 656s, 636s, 592m, 577m. Single crystals suitable for diffraction studies were obtained from the mother liquid.

### 2.2.2. Synthesis of $[\text{Ni}(\text{Pht})(\beta\text{-Pic})_2(\text{H}_2\text{O})_3] \cdot \text{H}_2\text{O}$ (**2**)

To a hot solution of KHPht (1.02 g, 5 mmol) and 3-methylpyridine (3 ml) in water (25 ml) was added a solution of  $\text{Ni}(\text{O}_2\text{CCH}_3) \cdot 4\text{H}_2\text{O}$  (1.24 g, 5 mmol) in water (10 ml). The resulting mixture was heated at reflux for 1.5 h and the resulting light green precipitate was collected from the hot solution by filtration. The filtrate was allowed to stand at r.t. in an open flask. The blue crystals of **2** suitable for X-ray diffraction studies were filtered off, washed with water and EtOH and dried in air. Yield: 0.67 g, 27.86%. *Anal. Calc.* for  $\text{C}_{20}\text{H}_{26}\text{N}_2\text{NiO}_8$ : C, 49.93; H, 5.45; N, 5.82. Found: C, 49.62; H, 5.51; N, 5.65%. IR data (KBr,  $\text{cm}^{-1}$ ): 3395s,br, 3071w,br, 1608sh, 1586sh, 1553vs, 1484m, 1449m, 1405vs, 1240w, 1196w, 1150w, 1130w, 1108w, 1086w, 1056w, 1037w, 820m, 793m, 757m, 702s, 653m, 562w. Single crystals suitable for diffraction studies were obtained from the mother liquid.

### 2.2.3. Synthesis of $[\text{Ni}(\text{Pht})(1\text{-MeIm})_2(\text{H}_2\text{O})_3]$ (**3**)

To a solution of  $[\text{Ni}(1\text{-MeIm})_6](\text{HPht})_2 \cdot 2\text{H}_2\text{O}$  (0.92 g, 0.1 mmol) in water (10 ml), a solution of  $\text{NiCl}_2 \cdot 6\text{H}_2\text{O}$  (0.24 g, 0.1 mmol) and KOH (0.06 g, 0.1 mmol) in water (10 ml) was added. The resulting solution was heated at reflux for two hours. Crystals of **3** suitable for X-ray diffraction studies crystallized after one month and were collected by filtration, washed with water and EtOH and dried in air. Yield: 0.56 g, 60.87%. *Anal. Calc.* for  $\text{C}_{16}\text{H}_{22}\text{N}_4\text{NiO}_7$ : C, 43.56; H, 5.03; N, 12.70. Found: C, 43.42; H, 4.94; N, 12.42%. IR data (KBr,  $\text{cm}^{-1}$ ): 3541sh, 3413m,br, 3147m, 1607sh, 1586sh, 1564s,

1481m, 1445m, 1399vs, 1286m, 1248m, 1229m, 1161w, 1112m, 1106m, 1027w, 943m, 828m, 749m, 720m, 683m, 664m, 653m, 617m, 574w.

## 2.3. X-ray crystallography

Experimental data were collected on a KUMA KM4CCD- $\kappa$ -axis diffractometer with a graphite monochromated Mo  $\text{K}\alpha$  radiation at 130 K for **1** and **3**. The crystals were positioned 60 mm from CCD camera. Six hundred and eighty two frames were measured for **1** and 782 frames for **3** (in six runs). The time of a single frame measurement was 30 and 4 s over  $0.75^\circ$   $\omega$ -scan for **1** and **3**, respectively. The absorption corrections were introduced by semi-empirical method from symmetry equivalent reflections [32] for **1**, the maximum and minimum transmission being 0.935 and 0.678, respectively. The data were processed using the KUMA diffraction (Wroclaw, Poland) program. For **2**, the intensity data were collected at 223 K on a Stoe Image Plate Diffraction System [33] using Mo  $\text{K}\alpha$  graphite monochromated radiation. Image plate distance 70 mm,  $\phi$  oscillation scans 0–200°, step  $\Delta\phi = 1.0^\circ$ . Crystal data and details of data collections and refinement for **1–3** are given in Table 1. The structures were solved by direct methods (SHELXS-97 [34]) and refined on  $F^2$  (SHELXL-97 [35]) in anisotropic approach for non-hydrogen atoms. The positions of H-atoms were located from the difference syntheses of electronic density and were refined in an isotropic approximation. Selected bond distances and angles are listed in Table 2.

## 2.4. Magnetic measurements

Magnetic susceptibility data of powdered samples were collected on a MPMS Quantum Design SQUID magnetometer (XL-5) in the temperature range of 300–1.8 K and at a field of 1000 G. The samples were placed in a gelatine capsule and a straw was used as the sample holder. The output data were corrected for the experimentally determined diamagnetism of the sample holder and the diamagnetism of the sample calculated from Pascal's constants. The Levenberg–Marquardt least-squares fitting algorithm, in combination with MAGPACK [36], was used to model the experimental magnetic susceptibility data.

## 3. Results and discussion

### 3.1. Synthesis and preliminary characterization

Reaction of nickel(II) acetate with *o*-phthalic acid and excess of pyridine in water resulted in the high yield formation of  $[\text{Ni}(\text{Pht})(\text{Py})_2(\text{H}_2\text{O})_3]$  (**1**). When nickel(II)

Table 1  
Crystal data and details of structural determinations

	1	2	3
Empirical formula	C <sub>18</sub> H <sub>20</sub> N <sub>2</sub> NiO <sub>7</sub>	C <sub>20</sub> H <sub>26</sub> N <sub>2</sub> NiO <sub>8</sub>	C <sub>16</sub> H <sub>22</sub> N <sub>4</sub> NiO <sub>7</sub>
Formula weight	435.07	481.14	441.09
Temperature (K)	130(2)	223(2)	130(2)
Wavelength (Å)	0.71073	0.71073	0.71073
Crystal size (mm)	0.6 × 0.5 × 0.15	0.5 × 0.35 × 0.2	0.6 × 0.3 × 0.3
Crystal system	monoclinic	monoclinic	triclinic
Space group	<i>P</i> 2 <sub>1</sub> / <i>n</i>	<i>P</i> 2 <sub>1</sub> / <i>c</i>	<i>P</i> $\bar{1}$
<i>a</i> (Å)	15.481(3)	7.666(1)	7.958(2)
<i>b</i> (Å)	7.272(1)	13.222(1)	9.244(2)
<i>c</i> (Å)	17.736(4)	21.813(2)	13.475(3)
$\alpha$ (°)	90	90	107.13(3)
$\beta$ (°)	105.00(3)	96.223(1)	95.87(3)
$\gamma$ (°)	90	90	98.20(3)
<i>U</i> (Å <sup>3</sup> )	1928.6(6)	2198.0(3)	926.6(4)
<i>Z</i>	4	4	2
<i>D</i> <sub>c</sub> (g cm <sup>-3</sup> )	1.498	1.454	1.581
$\mu$ (mm <sup>-1</sup> )	1.049	0.931	1.095
<i>F</i> (0 0 0)	904	1008	460
$\theta$ Range for data collection (°)	3.68–29.60	2.43–25.90	3.18–26.37
Index ranges	–20 ≤ <i>h</i> ≤ 20, –9 ≤ <i>k</i> ≤ 8, –23 ≤ <i>l</i> ≤ 23	–9 ≤ <i>h</i> ≤ 9, –16 ≤ <i>k</i> ≤ 16, –26 ≤ <i>l</i> ≤ 26	–9 ≤ <i>h</i> ≤ 9, –11 ≤ <i>k</i> ≤ 10, –16 ≤ <i>l</i> ≤ 15
Reflections collected	15 413	16 614	7358
Reflections unique [ <i>R</i> <sub>int</sub> ]	4934 [0.0278]	4228 [0.0662]	3758 [0.0672]
Completeness to $\theta_{\max}$	91.0	99.1	99.1
Data/restraints/parameters	4934/0/334	4228/0/384	3758/0/341
Final <i>R</i> indices [ <i>I</i> > 2 $\sigma$ ( <i>I</i> )]	<i>R</i> <sub>1</sub> = 0.0270, <i>wR</i> <sub>2</sub> = 0.0657	<i>R</i> <sub>1</sub> = 0.0340, <i>wR</i> <sub>2</sub> = 0.0815	<i>R</i> <sub>1</sub> = 0.0350, <i>wR</i> <sub>2</sub> = 0.0913
<i>R</i> indices (all data)	<i>R</i> <sub>1</sub> = 0.0296, <i>wR</i> <sub>2</sub> = 0.0675	<i>R</i> <sub>1</sub> = 0.0448, <i>wR</i> <sub>2</sub> = 0.0860	<i>R</i> <sub>1</sub> = 0.0397, <i>wR</i> <sub>2</sub> = 0.0939
Goodness-of-fit on <i>F</i> <sup>2</sup>	1.025	0.978	1.097
Largest difference peak and hole (e Å <sup>-3</sup> )	0.389 and –0.406	0.806 and –0.394	0.417 and –0.846

acetate reacted with KHPht and excess  $\beta$ -Pic light, a light green precipitate was initially formed. According to elemental analysis and IR spectrum, this precipitate corresponds to [Ni(Pht)( $\beta$ -Pic)(H<sub>2</sub>O)].<sup>1</sup> Concentration of the filtrate by evaporation gave complex **2**, [Ni(Pht)( $\beta$ -Pic)<sub>2</sub>(H<sub>2</sub>O)<sub>3</sub>] · H<sub>2</sub>O, in low yield (27%). Complex **3**, [Ni(Pht)(1-MeIm)<sub>2</sub>(H<sub>2</sub>O)<sub>3</sub>], is prepared in high yield (60.87%) by the reaction of nickel(II) salt with [Ni(1-MeIm)<sub>6</sub>](HPht)<sub>2</sub> · 2H<sub>2</sub>O.

The IR spectra of compounds **1–3** show characteristic bands of carboxylate groups in the usual region 1608–1553 cm<sup>-1</sup> for asymmetric stretching and in 1405–1399 cm<sup>-1</sup> region for symmetric stretching. Their positions and intensities are similar to those reported for other phthalates [1,3,8,14,15,28] and carboxylate complexes [37–39]. The infrared spectra also show broad bands in the 3541–3071 cm<sup>-1</sup> region, which can be assigned to water molecules.

The thermogravimetric analyses of compounds **1** and **2** indicated a sharp mass loss, followed by a long tail,

<sup>1</sup> Anal. Calc. for C<sub>14</sub>H<sub>13</sub>NNiO<sub>5</sub>: C, 50.35; H, 3.92; N, 4.19. Found: C, 50.60; H, 3.76; N, 4.16%. IR data (KBr, cm<sup>-1</sup>): 3411s,br, 1642vs, 1610vs, 1589sh, 1562vs, 1488s, 1446s, 1415vs, 1199w, 1163w, 1131w, 1112w, 1086w, 1060m, 1038m, 859m, 822s, 792m, 769m, 748m, 697s, 655s, 469w.

Table 2  
Selected bond distances (Å) and bond angles (°)

	1	2	3
Ni(1)–O(4)	2.010(1)	2.053(1)	2.036(2)
Ni(1)–N(1A)	2.066(1)	2.106(2)	2.054(2)
Ni(1)–N(1B)	2.073(1)	2.099(2)	2.076(2)
Ni(1)–O(1w)	2.078(1)	2.069(2)	2.110(1)
Ni(1)–O(2w)	2.126(1)	2.077(2)	2.128(2)
Ni(1)–O(3w)	2.075(1)	2.095(2)	2.080(2)
O(4)–Ni(1)–N(1A)	170.95(4)	170.35(6)	176.93(5)
O(4)–Ni(1)–N(1B)	91.70(5)	92.45(6)	89.31(6)
O(4)–Ni(1)–O(1w)	85.59(4)	84.31(6)	82.56(6)
O(4)–Ni(1)–O(2w)	83.13(4)	85.76(6)	83.25(6)
O(4)–Ni(1)–O(3w)	92.56(4)	91.66(6)	90.51(6)
N(1A)–Ni(1)–N(1B)	90.59(5)	95.66(6)	93.60(7)
N(1A)–Ni(1)–O(1w)	92.28(5)	87.72(6)	94.51(7)
N(1A)–Ni(1)–O(3w)	96.16(5)	94.11(7)	90.51(6)
N(1A)–Ni(1)–O(2w)	88.01(4)	89.24(7)	95.70(6)
N(1B)–Ni(1)–O(1w)	177.02(4)	176.38(6)	171.81(6)
N(1B)–Ni(1)–O(3w)	90.61(4)	86.14(6)	89.31(6)
N(1B)–Ni(1)–O(2w)	92.93(4)	88.34(6)	91.06(6)
O(1w)–Ni(1)–O(2w)	88.00(4)	93.02(6)	87.05(6)
O(3w)–Ni(1)–O(1w)	88.26(4)	92.33(6)	91.71(6)
O(3w)–Ni(1)–O(2w)	174.50(4)	173.80(6)	173.74(5)

with total mass loss of 82.88% and 84.59% in the range 25–450 °C, which is in agreement with the mass loss calculated for the loss of both water molecules and organic

moieties (Calc. 82.78% and 84.43%). For compound **3**, a mass loss of 12.28% in the 25–130 °C temperature range corresponds to the loss of three coordinated water molecules for the formula units (Calc. 12.26%) and the second mass loss of 69.49% corresponds to the loss of the organic moieties (Calc. 70.76%).

### 3.2. Crystal structures

The structures of compounds **1–3** (Fig. 1(a)–(c)) are similar to structures of molecular compounds with monodentate coordination mode of one carboxylate

group of *o*-phthalic acid [24–28]. In all three compounds, nickel atoms have octahedral coordination geometry. Two *cis*-positions in the coordination polyhedron are occupied by two nitrogen atoms of aromatic amines with the Ni–N distances of 2.066(1) and 2.073(1) Å (**1**), 2.099(2) and 2.106(2) Å (**2**), and 2.054(2) and 2.076(2) Å (**3**). The dihedral angle between the aromatic rings is 117.2(2)° for **1**, 106.6(2)° for **2** and 90.1(2)° for **3**. The phthalate ligand is coordinated to the nickel atom in a monodentate fashion and occupies one place in the octahedron with bond distances Ni–O(4) = 2.010(1), 2.053(1) and 2.036(2) Å for **1–3**,

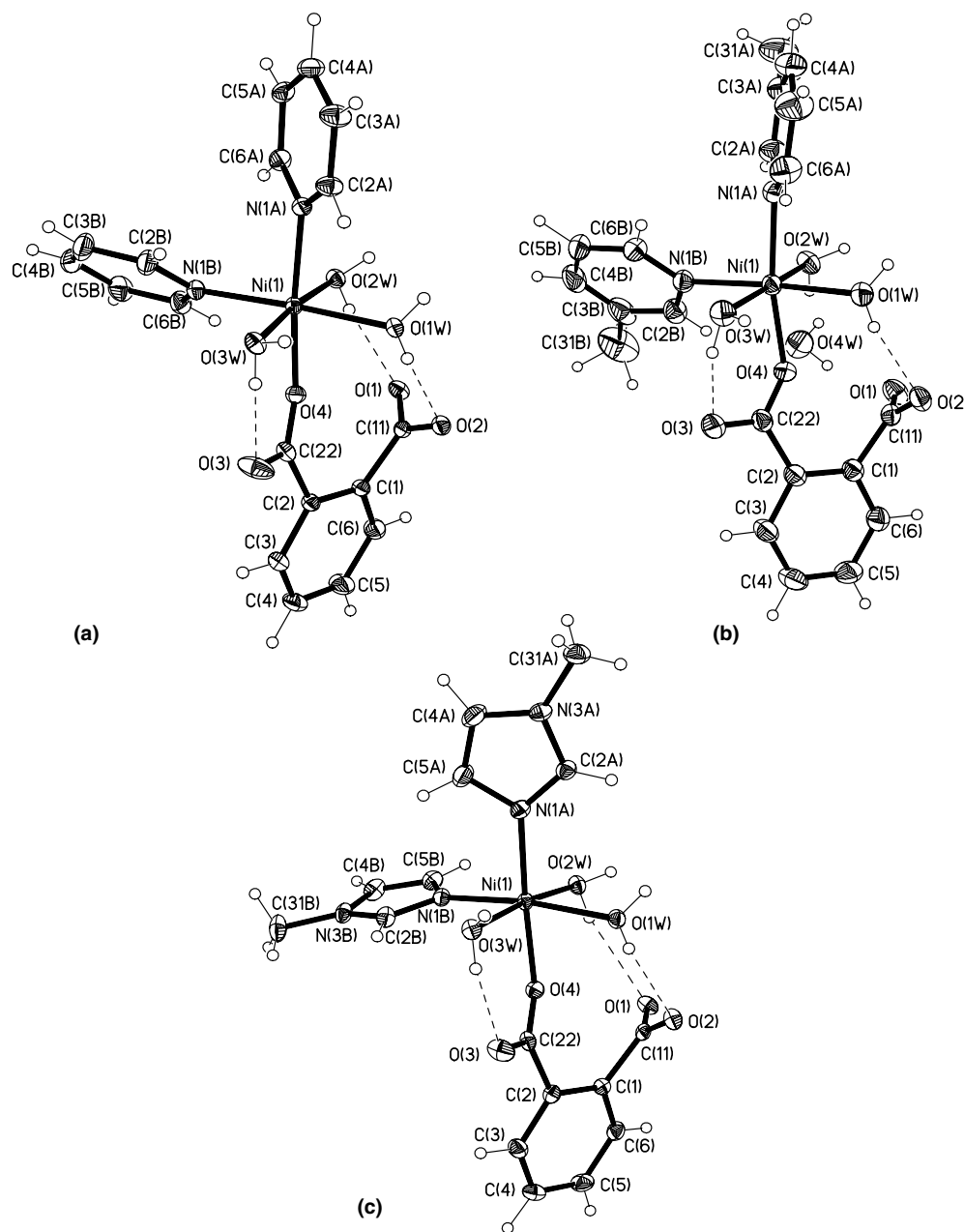


Fig. 1. Crystallographically independent structure fragments with numbering scheme and displacement ellipsoids drawn at the 50% probability level in compounds  $[\text{Ni}(\text{Pht})(\text{Py})_2(\text{H}_2\text{O})_3]$  (**1a**),  $[\text{Ni}(\text{Pht})(\beta\text{-Pic})_2(\text{H}_2\text{O})_3] \cdot \text{H}_2\text{O}$  (**1b**) and  $[\text{Ni}(\text{Pht})(1\text{-MeIm})_2(\text{H}_2\text{O})_3]$  (**1c**).

respectively. Finally, the coordination sphere is completed by oxygen atoms of three water molecules. The Ni–O(w) distances vary in the range of 2.069(2)–2.128(2) Å (Table 2).

The presence of water molecules and carboxyl groups makes extensive hydrogen bonding interactions in compounds **1–3**, which are listed in Table 3. Fig. 1(a)–(c) illustrates intramolecular hydrogen bonds of O(w)–H···O type in these compounds. They are identical for **1** and **3** and differ slightly for **2** by reason of presence of the solvate water molecule O(4w).

The water molecule O(3w) and carboxylate oxygen atom O(3) form the hydrogen bond O(3w)–H···O(3) = 2.714(2) Å (**1**), 2.753(2) Å (**2**), and 2.664(2) Å (**3**), leading to the organization of the six-membered Ni(1)–O(3w)–H···O(3)–C(22)–O(4)–Ni(1) hydrogen bonded ring. The coordinated water molecules O(1w) and O(2w) take part in the formation of 9-membered hydrogen bonded rings Ni(1)–O(1w)–H···O(2)–C(11)–C(1)–C(2)–C(22)–O(4)–Ni(1) in all title compounds and Ni(1)–O(2w)–H···O(1)–C(11)–C(1)–C(2)–C(22)–O(4)–Ni(1) only in **1** and **3**. The corresponding distances are 2.830(2) (**1**), 2.906(2) Å (**2**) and 2.917(2) Å (**3**), and O(2w)–H···O(1) distances are 2.993(2) and 3.316(2) Å for **1** and **3**, respectively. In **2**, the water molecule O(2w) is only involved in intermolecular H-bonding (Fig. 1(b), Table 3). Similar intramolecular hydrogen bonding pattern was observed in the structures of all hy-

drated Ni(II) complexes with monocoordinated *o*-phthalic acid.

Interestingly, the intermolecular O(w)–H···O(carb.) hydrogen interactions are very important in the construction of the crystal edifice of **1–3**. In compound **1**, water molecules O(1w) and O(2w) are involved in both the formation of intramolecular *pseudo*-cycles with O(1) and O(2) oxygen atoms of phthalate carboxylate groups and the hydrogen bonding with identical oxygen atoms on the adjacent complex (symmetry code [ $-x - 2, -y - 1, -z$ ]) (Table 3). As a consequence, individual molecules are joined into centrosymmetric dimers as shown in Fig. 2(a) with M···M distances of 6.570(1) Å. Hydrogen bonds O(3w)–H···O(1) connect adjacent dimers in double-chains along the *y*-axis of the unit cell of **1** (Fig. 2(b)). Distance between metals of the adjacent dimers is 7.272(1) Å. In compounds **2** and **3**, water molecules O(1w), O(2w) and O(3w) adopt the same role and form analogous double chains. The M···M distances in the dimers are 6.421(1) Å for **2** and 6.930(1) Å for **3**, and between dimers are 7.666(1) and 7.958(1) Å for **2** and **3**, respectively. The solvate molecule O(4w) in **2** gives rise to hydrogen bonds only inside the double-chain. Furthermore, similar double-chains are observed in all the above noted Ni-compounds with monodentate phthalates [24–28]. Depending on the nature of aromatic amines, the arrangement of these chains differs between crystals. The double-chains are held together only by

Table 3  
Hydrogen bonding interaction in the crystal structures **1–3**

D–H···A	Symmetry operation generating A	Distances (Å)			Angles (°)
		D–H	H···A	D···A	
<i>Compound 1</i>					
O(1w)–H(1w2)···O(1)	$-x - 2, -y - 1, -z$	0.80(2)	1.89(3)	2.693(2)	174(2)
O(1w)–H(1w1)···O(2)		0.83(2)	2.00(2)	2.830(2)	176(2)
O(2w)–H(2w1)···O(1)		0.80(2)	2.20(2)	2.993(2)	171(2)
O(2w)–H(2w2)···O(2)	$-x - 2, -y - 1, -z$	0.82(3)	1.97(3)	2.785(1)	178(2)
O(3w)–H(3w2)···O(3)		0.81(2)	1.92(2)	2.714(2)	166(2)
O(3w)–H(3w1)···O(1)	$x, y - 1, z$	0.86(2)	1.91(2)	2.765(1)	174(2)
<i>Compound 2</i>					
O(1w)–H(1w2)···O(1)	$-x, -y + 1, -z$	0.87(3)	1.83(3)	2.699(2)	177(3)
O(1w)–H(1w1)···O(2)		0.81(3)	2.11(3)	2.906(2)	168(2)
O(2w)–H(2w1)···O(4w)		0.87(3)	1.96(3)	2.817(2)	169(2)
O(2w)–H(2w2)···O(2)	$-x, -y + 1, -z$	0.85(4)	1.86(4)	2.700(2)	170(4)
O(3w)–H(3w2)···O(3)		0.91(3)	1.87(3)	2.753(2)	161(3)
O(3w)–H(3w1)···O(2)	$-x + 1, -y + 1, -z$	0.84(3)	1.92(3)	2.723(2)	157(3)
O(4w)–H(4w1)···O(1)		0.87(4)	1.92(4)	2.757(2)	162(3)
O(4w)–H(4w2)···O(3)	$x - 1, y, z$	0.90(3)	1.87(3)	2.755(2)	169(3)
<i>Compound 3</i>					
O(1w)–H(1w1)···O(1)	$-x + 1, -y + 1, -z$	0.82(3)	1.90(3)	2.711(2)	168(3)
O(1w)–H(1w2)···O(2)		0.76(3)	2.17(3)	2.917(2)	170(3)
O(2w)–H(2w2)···O(2)	$-x + 1, -y + 1, -z$	0.79(3)	1.93(3)	2.716(2)	172(3)
O(2w)–H(2w1)···O(1)		0.87(3)	2.47(3)	3.316(2)	163(2)
O(3w)–H(3w2)···O(1)	$x - 1, y, z$	0.78(3)	2.00(3)	2.776(2)	175(3)
O(3w)–H(3w1)···O(3)		0.82(3)	1.89(3)	2.664(2)	158(3)

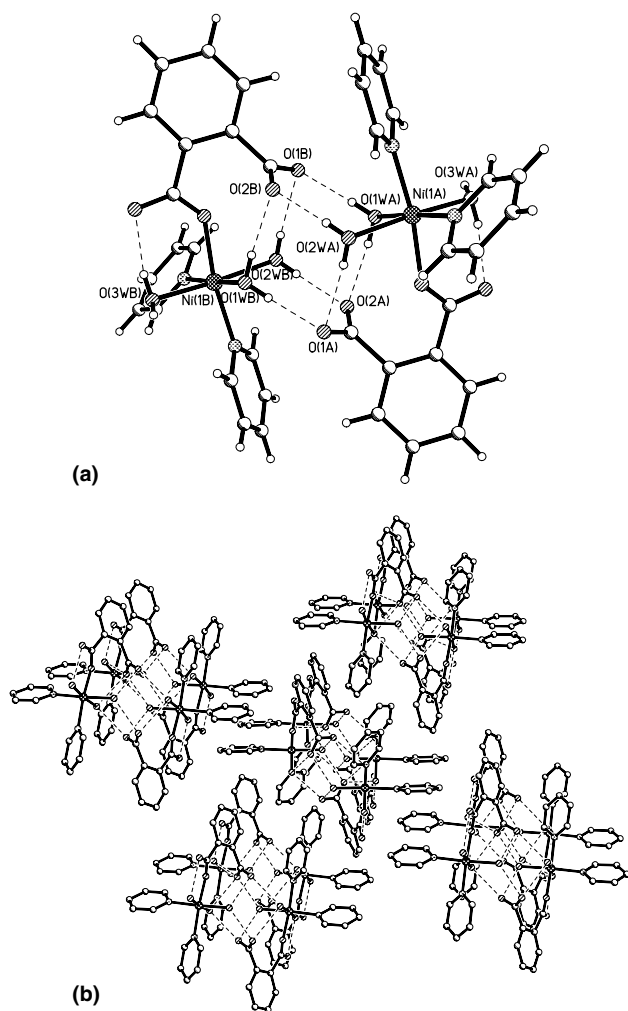


Fig. 2. (a) The hydrogen bonded centrosymmetric dimer in **1**. (b) The view of double-chains in this compound. Hydrogen atoms are omitted for the sake of clarity and hydrogen bonds are indicated by dotted lines.

van der Waals interactions in compound **1** (Fig. 3). In contrast, in **2** these chains form layers parallel to the  $y$ -axis by  $\pi$ - $\pi$  interactions between antiparallel molecules of  $\beta$ -Pic (Fig. 4) with an average distance between aromatic rings of 3.38 Å and a centroid-centroid distance of 3.791(2) Å. In addition, the layers are inter-linked together into a network by  $\pi$ - $\pi$  interactions between  $\beta$ -Pic and Pht rings, the average contact distance of two adjacent aromatic rings is about 3.48 Å and the centroid-centroid distance is 3.868(2) Å. The dihedral angle between the aromatic rings is 7.2(2)°. In complex **3**, the double-chains are knitted together via C(31b)-H $\cdots$ O(4)  $[-x+1, -y+1, -z+1]$  hydrogen bonds of 3.342(3) Å between the methyl group of 1-MeIm and the coordinated carboxylate oxygen atom, as well as  $\pi$ - $\pi$  contacts involving antiparallel 1-MeIm cycles (centroid-centroid distance is 3.719(3) Å) to build up layers parallel to the  $xz$ -plane as depicted in Fig. 4.

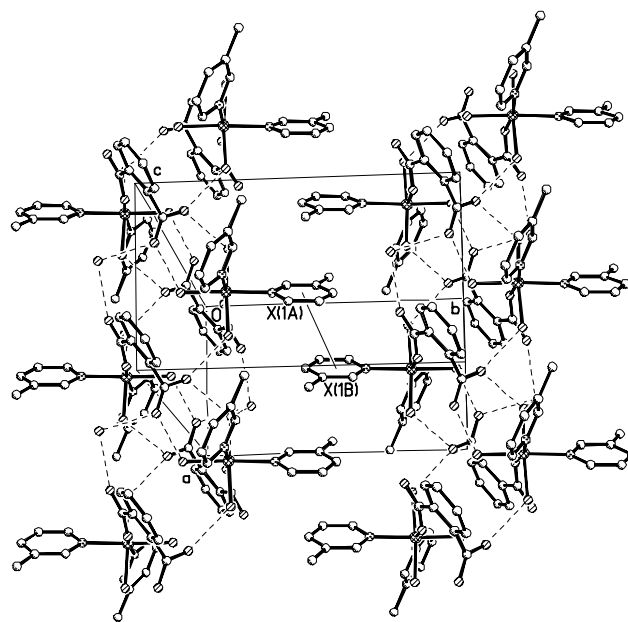


Fig. 3. Fragment of the crystal structure of compound **2** showing the double chains formed by hydrogen bonding and  $\pi$ -stacking interaction between them (centroid-centroid distance X(1A)-X(1B) is equal 3.791(2) Å).

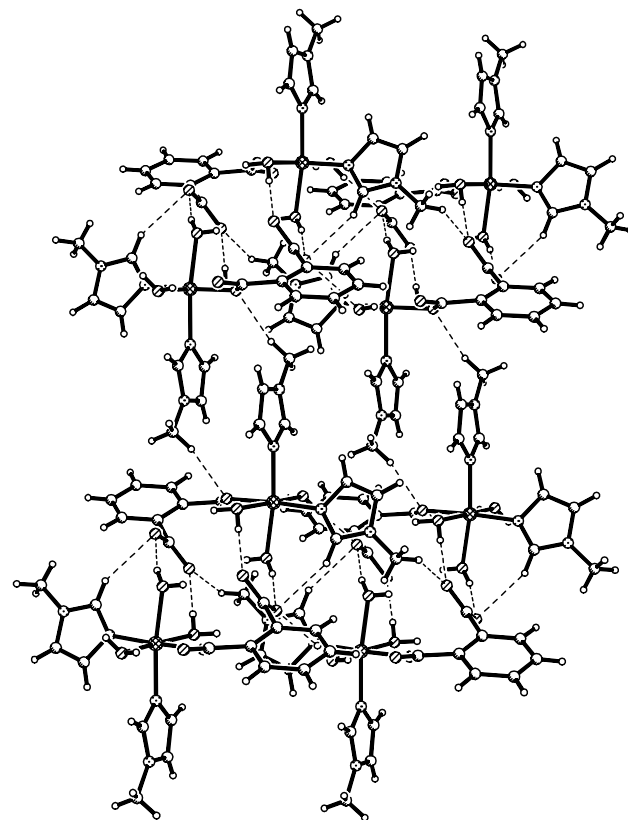


Fig. 4. Crystal packing perspective view of **3** showing supramolecular weak aromatic  $\pi$ - $\pi$  stacking interactions and C-H $\cdots$ O hydrogen-bonding.

#### 4. Magnetic properties

The thermal dependence of  $\chi_M T$  ( $\chi_M T$  being the product of the molar magnetic susceptibility and the temperature) and the simulated curves for powdered samples of the hydrogen bonded dimeric nickel compounds 1–3 are shown in Figs. 5–7. The molar magnetic susceptibilities have been corrected for their diamagnetic and temperature independent paramagnetic (TIP) contributions. For compound 1, the TIP is  $9 \times 10^{-4}$  emu/mol. The  $\chi_M T$  values remain essentially constant at 2.45 emu K/mol between 300 and 100 K. This value agrees well with the expected 2.42 emu K/mol for two uncoupled  $\text{Ni}^{2+}$  ions with  $S = 1$  and  $g = 2.2$ . Below 100 K,  $\chi_M T$  decreases due to zero-field splitting and weak antiferromagnetic interaction between the  $\text{Ni}^{2+}$  ions. The simulation with a  $g$ -value of 2.22, an axial zero-field splitting parameter  $|D| = 4.11 \text{ cm}^{-1}$  and an antiferromagnetic interaction parameter  $J = -0.29 \text{ cm}^{-1}$ , agreed best with the experimental data. Similarly, the  $\chi_M T$  values of compound 2 (TIP =  $9 \times 10^{-4}$  emu/mol) remain constant at 2.47 emu K/mol down to 100 K and decrease at lower temperatures. A simulation of the magnetic data for this compound resulted in  $g = 2.215$ ,  $|D| = 3.85 \text{ cm}^{-1}$  and  $J = -0.1 \text{ cm}^{-1}$ . For compound 3 (TIP =  $9.6 \times 10^{-4}$  emu/mol), the experimental value of  $\chi_M T$  is 2.50 emu K/mol at room temperature. In contrast to compounds 1 and 2, the values of  $\chi_M T$  of compound 3 increase below 100 K, suggesting ferromagnetic interaction between the  $\text{Ni}^{2+}$  ions. These data could be simulated best with the corresponding parameters  $g = 2.23$ ,  $J = 0.22 \text{ cm}^{-1}$  and  $|D| = 4.6 \text{ cm}^{-1}$ . Overall, all three compounds exhibit weak magnetic exchange interactions and subtle structural differences may cause a

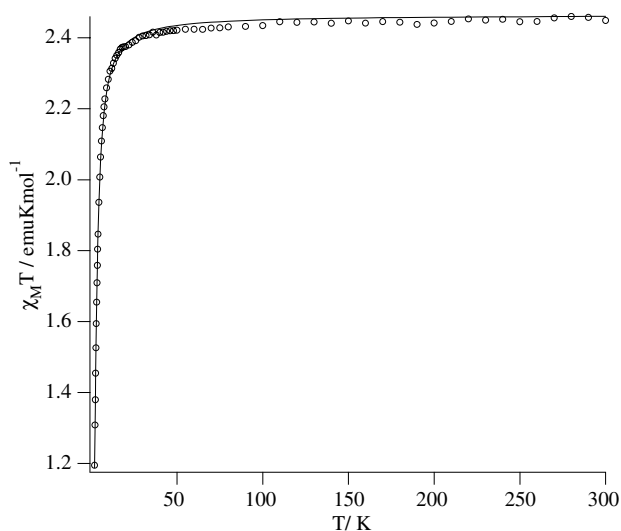


Fig. 5. Temperature dependence of  $\chi_M T$  for compound 1. The circles correspond to the experimental data, the simulation is depicted as a line.

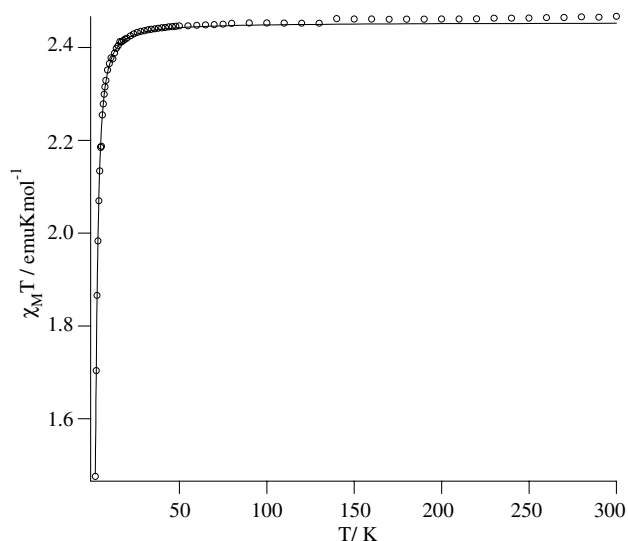


Fig. 6. Temperature dependence of  $\chi_M T$  for compound 2. The circles correspond to the experimental data, the simulation is depicted as a line.

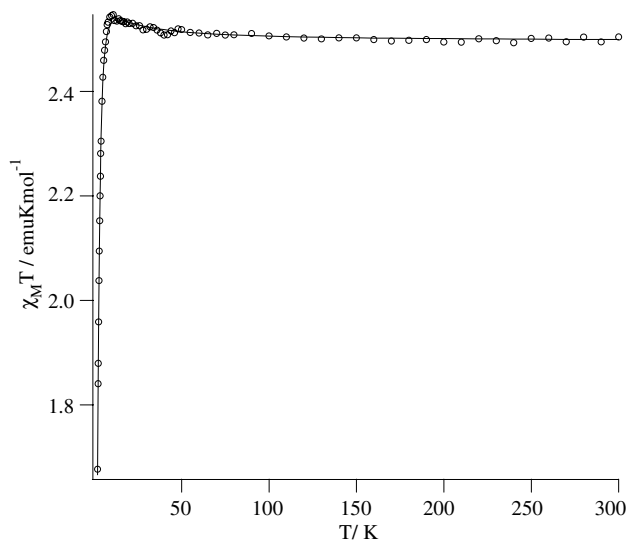


Fig. 7. Temperature dependence of  $\chi_M T$  for compound 3. The circles correspond to the experimental data, the simulation is depicted as a line.

change from a total antiferromagnetic interaction to a ferromagnetic type of interaction as it is seen for compound 3. However, the structural aspects are too complex to render a conclusive structure–property relation.

#### 5. Supplementary material

Crystallographic data for the structural analysis have been deposited with the Cambridge Crystallographic Data Centre, CCDC nos. 232778 (1), 232777 (2) and 232776 (3). Copies of this information may be obtained

from The Director, CCDC, 12 Union Road, Cambridge, CB2 1EZ, UK (fax: +44 1233 336033; e-mail: deposit@ccdc.cam.ac.uk or www: <http://www.ccdc.cam.ac.uk>).

### Acknowledgment

This work was supported by the Swiss National Science Foundation (SCOPES 7MDPJ065712.01/1).

### References

- [1] S.G. Baca, I.G. Filippova, O.A. Gherco, M. Gdaniec, Yu.A. Simonov, N.V. Gerbeleu, P. Franz, R. Basler, S. Decurtins, *Inorg. Chim. Acta* 357 (2004) 3419.
- [2] F.H. Allen, *Acta Crystallogr., Sect. B* 58 (2002) 380.
- [3] S.G. Baca, Yu.A. Simonov, M. Gdaniec, N.V. Gerbeleu, I.G. Filippova, G.A. Timco, *Inorg. Chem. Commun.* 6 (2003) 685.
- [4] M.B. Cingi, C. Guastini, A. Musati, N. Nardelli, *Acta Crystallogr., Sect. B* 26 (1970) 1836.
- [5] (a) M.B. Cingi, A.M.M. Lanfredi, A. Tiripicchio, M.T. Camellini, *Acta Crystallogr., Sect. B* 33 (1977) 659;  
(b) M.B. Cingi, A.M.M. Lanfredi, A. Tiripicchio, M.T. Camellini, *Acta Crystallogr., Sect. B* 34 (1978) 412.
- [6] I. Krstanovic, Lj. Karanovic, Dj. Stojakovic, *Acta Crystallogr., Sect. C* 41 (1985) 43.
- [7] B.L. Rodrigues, M.D.D. Costa, N.G. Fernandes, *Acta Crystallogr., Sect. C* 55 (1999) 1997.
- [8] (a) N.V. Gerbeleu, Yu.A. Simonov, G.A. Timco, P.N. Bourosh, J. Lipkowski, S.G. Baca, D.I. Saburov, M.D. Mazus, *Russ. J. Inorg. Chem.* 44 (1999) 1191;  
(b) S.G. Baca, S.T. Malinovskii, P. Franz, Ch. Ambrus, H. Stoeckli-Evans, N. Gerbeleu, S. Decurtins, *J. Solid State Chem.* 177 (2004) 2841.
- [9] Y. Zhang, J. Li, Q. Su, Q. Wang, X. Wu, *J. Mol. Struct.* 516 (2000) 231.
- [10] P. Lightfoot, A. Snedden, *J. Chem. Soc., Dalton Trans.* (1999) 3549.
- [11] E. Suresh, K. Boopalan, R.V. Jasra, M.M. Bhadbhade, *Inorg. Chem.* 40 (2001) 4078.
- [12] Yu.A. Simonov, M. Gdaniec, I.G. Filippova, S.G. Baca, G.A. Timco, N.V. Gerbeleu, *Russ. J. Coord. Chem.* 27 (2001) 353.
- [13] A.D. Burrows, R.W. Harrington, M.F. Mahon, C.E. Price, *J. Chem. Soc., Dalton Trans.* (2000) 3845.
- [14] S.G. Baca, Yu.A. Simonov, N.V. Gerbeleu, M. Gdaniec, P.N. Bourosh, G.A. Timco, *Polyhedron* 20 (2001) 831.
- [15] S.G. Baca, I.G. Filippova, N.V. Gerbeleu, Yu.A. Simonov, M. Gdaniec, G.A. Timco, O.A. Gherco, Yu.L. Malaestean, *Inorg. Chim. Acta* 344 (2003) 109.
- [16] J.W. Bats, A. Kallel, H. Fuess, *Acta Crystallogr., Sect. B* 34 (1978) 1705.
- [17] R.C. Squire, S.M.J. Aubin, K. Folting, W.E. Streib, D.N. Hendrickson, G. Christou, *Angew. Chem. Int., Ed. Engl.* 34 (1995) 887.
- [18] R.C. Squire, S.M.J. Aubin, K. Folting, W.E. Streib, G. Christou, D.N. Hendrickson, *Inorg. Chem.* 34 (1995) 6463.
- [19] C. Cañada-Vilalta, M. Pink, G. Christou, *J. Chem. Soc., Dalton Trans.* (2003) 1121.
- [20] E.K. Brechin, R.O. Gould, S.G. Harris, S. Parsons, R.E.P. Winpenny, *J. Am. Chem. Soc.* 118 (1996) 11293.
- [21] E.K. Brechin, S.G. Harris, S. Parsons, R.E.P. Winpenny, *J. Chem. Soc., Chem. Commun.* (1996) 1439.
- [22] E.K. Brechin, A. Graham, A. Parkin, S. Parson, A.M. Seddon, R.E.P. Winpenny, *J. Chem. Soc., Dalton Trans.* (2000) 3242.
- [23] G.B. Shul'pin, G. Süß-Fink, L.S. Shul'pina, *J. Mol. Catal.* 170 (2001) 17.
- [24] G. Adiwidjaja, H. Kupperts, *Acta Crystallogr., Sect. B* 32 (1976) 1571.
- [25] N.P. Kozlova, V.M. Agre, V.K. Trunov, S.S. Makarevich, N.N. Barkhanova, *Russ. J. Struct. Chem.* 23 (1982) 108.
- [26] D. Poleti, D.R. Stojakovic, B.V. Prelesnik, Lj. Manojlovic-Muir, *Acta Crystallogr., Sect. C* 46 (1990) 399.
- [27] D. Poleti, L. Karanovic, B.V. Prelesnik, *Acta Crystallogr., Sect. C* 46 (1990) 2465.
- [28] F.-C. Xue, Z.-H. Jiang, D.-Z. Liao, S.-L. Ma, S.-P. Yan, G.-L. Wang, X.-K. Yao, R.-J. Wang, *Polyhedron* 12 (1993) 2787.
- [29] H. Endres, *Z. Anorg. Allg. Chem.* 513 (1984) 78.
- [30] M.B. Cingi, A.M.M. Lanfredi, A. Tiripicchio, *Acta Crystallogr., Sect. C* 40 (1984) 56.
- [31] Z. Tomic, B. Prelesnik, L. Karanovic, D. Poleti, *J. Serb. Chem. Soc.* 61 (1996) 97.
- [32] XEMP Ver. 4.2 Siemens Analytical X-ray Inst. Inc., 1990.
- [33] Stoe & Cie IPDS Software. Stoe & Cie GmbH, Darmstadt, Germany, 2000.
- [34] G.M. Sheldrick, *SHELXS-97* Program for the Solution of Crystal Structures, University of Goettingen, Germany, 1997.
- [35] G.M. Sheldrick, *SHELXL-97*, Program for the Refinement of Crystal Structures, University of Goettingen, Germany, 1997.
- [36] J.J. Borrás-Almenar, J.M. Clemente-Juan, E. Coronado, B.S. Tsukerblatt, *Inorg. Chem.* 38 (1999) 6081.
- [37] G.B. Deacon, R.J. Phillips, *Coord. Chem. Rev.* 33 (1980) 227.
- [38] K. Nakamoto, *Infrared and Raman Spectra of Inorganic and Coordination Compounds*, Wiley, New York, 1986, p. 236.
- [39] R.C. Mehrotra, R. Bohra, *Metal Carboxylates*, Academic Press, New York, 1983, p. 48.